Direct observation of atom movement in photoexcited ionic-electronic conductors

Yasushi Utsugi*
NTT Laboratories, 3-1 Morinosato Wakamiya, Atsugi 243-01, Japan
(Received 24 May 1996; revised manuscript received 22 November 1996)

An analysis of the topological, optical, and chemical characteristics of pattern-photoexposed ionic-electronic conductor Ag_2Se surfaces has revealed a very interesting phenomenon: the formation of hills 100–500 Å in height on the exposed Ag_2Se/Ge-Se surface area. The hills are a result of pressure caused by the production of Ag metal clusters at the photoexposed Ag_2Se surface, which results in a four-layer structure of (Ag metal)/Ag_2Se/(Ag-doped Ge-Se)/Ge-Se. The Ag hill formation plays a more dominant role in Ag lateral diffusion than Ag photodoping does. [S0163-1829(97)01216-2]

I. INTRODUCTION

Currently, there is considerable interest in understanding the dynamics of the electron-excited rearrangement of atoms in condensed materials.[1] There appears to be remarkable atom movement with low excitation energy in nonequilibrium materials and ionic conductors. In fact, chalcogenide glasses, which are typical nonequilibrium materials, are famous for showing photostructural changes, and silver chalcogenides, which are typical ionic conductors, are known to be chemically modified by external excitation.[2,3] Silver selenide, Ag_2Se, is an ionic-electronic conductor containing many mobile atoms that interact with electrons. When it is formed on top of Ge-Se glasses, exceptional photoexcited atom movement in the form of Ag photodoping to the Ge-Se matrix and Ag lateral diffusion in the Ag_2Se matrix has been observed.[4] Because these phenomena are so remarkable in this system, it has been successfully applied as a photoresist for lithography and as an x-ray plate.[5,6] Studies of Ag-atom behavior commonly hold that the Ag lateral diffusion results from vertical Ag migration, and that a horizontally sharp Ag-doped profile in the Ge-Se matrix is resultantly induced at the exposure edge (edge sharpening).[4,7,8] However, a critical problem remains in these descriptions: the edge sharpening is no more than the result of calculations assuming that Ag migrates only on the exposed region. Our work, on the other hand, is concerned with the experimental verification of an intermingling of some atom transport mechanisms.

This paper shows that photoirradiation results in the formation of ''Ag metal mounds'' on the surface at the exposure edges. This means that photoexcitation of the Ag_2Se/Ge-Se system causes a heretofore unknown type of vertical atom movement and changes the systems' structure into a four-layer one comprising (Ag metal)/Ag_2Se/(Ag-doped Ge-Se)/Ge-Se, as opposed to simply causing atom rearrangements.

II. EXPERIMENT

First 200-nm-thick $GeSe_4$ films were deposited on polished mirrorlike silicon wafers or silicate glasses. Silver sensitization was carried out by chemically plating Ag on the film to produce Ag_2Se compounds (about 20 nm thick) and form the $Ag_2Se/GeSe_4$ structure.[5] For patterned photoexposures on the Ag_2Se surface, contact printing was done through a partially Cr-coated glass photomask with various aerial line and space (L/S) patterns. The width of the lines and spaces ranged from 3 to 500 μm. An i-line light (wavelength: $\lambda = 365$ nm) from a high-pressure mercury lamp was used for the exposure (100–5000 mJ/cm^2).

Pattern-exposed surfaces were measured to assess their topological, optical, and chemical characteristics. The surfaces just after the exposure were measured with a scanning electron microscope (SEM) and a stylus-type profiler to study changes in surface topology. The SEM was principally used to study horizontal effects on the exposed surface, and we were able to obtain exact vertical-surface profiles with the profiler. The stylus has a radius of 1 μm at the end, which gives high horizontal resolution. The measurement was done under a stylus load of 1 dyn, and with a vertical resolution of 10 Å at maximum.

Besides observing the usual transparent images of the surface with an ordinary optical microscope, we also measured reflectance line profiles from the pattern-exposed surfaces. The measurements were conducted by scanning the He-Ne laser beam over the surface, and by synchronously recording the reflected light. The laser beam was focused to 0.8 μm in diameter through some lenses, and was projected normally to the surface. It was then scanned over the surface across the direction of exposed L/S pattern once. The normally reflected light from the surface, detected by a Si photodiode, was recorded synchronously with a memory oscilloscope. To avoid damaging the pattern-exposed surface with the laser beam, the scan was done very quickly (1 μm/ms). This technique could provide the reflectance line profiles in high spatial resolution superior to 1 μm. A detailed description of the measurement system will be given elsewhere.

The chemical composition on the pattern-exposed surface was analyzed by Auger electron spectroscopy (AES) at 10-keV excitation with a cylindrical mirror analyzer. The angle between the surface and the impinging-electron direction was 60°. To determine the precise surface distribution of Ag, Se, and Ge elements, AES surface images and line profiles were measured for Ag-*MNN* (356 eV), Se-*LMM* (1315 eV), and Ge-*LMM* (1147 eV) transition lines, respectively. The measurements were conducted by scanning the impinging-electron beam, which was 500 Å in diameter.

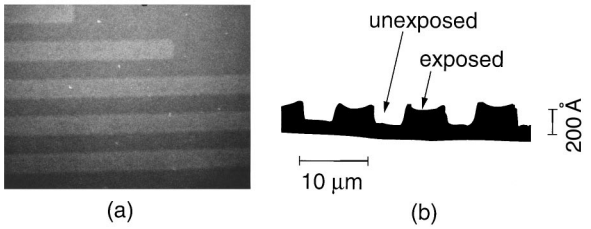

FIG. 1. (a) A SEM photograph of the $Ag_2Se/GeSe_4$ surface just after exposure (4000 mJ/cm^2) with aerial lines (5 μm wide) and spaces (5 μm wide). (b) The profile of the surface in (a) is measured with a stylus-type profiler.

III. RESULTS

Our first observations of the anomalous topological effects are shown in Fig. 1 Figure 1(a) shows a typical SEM image of the surface just after patterned exposure. The brighter parts are exposed areas, and the shaded parts are unexposed areas. The obtained image should show the chemical and/or topological features over the entire surface. The surface was uniformly coated with a Pd-Ag alloy (10 nm thick) to exclude any effects due to changes in the chemical composition from the SEM image. In this case, we also obtained a SEM surface image, in which pattern boundaries were clear. Therefore, we can assert that patterned photoexposure causes both changes in the chemical composition and topology of the surface. Figure 1(b) shows a typical topological profile of the surface, measured with a stylus-type profiler. The photoexposed regions rise to a height of several hundred Å and the profiles, once formed, never disappear or collapse. It is noteworthy that the raised regions, or mounds, have various shapes, depending on exposure intensity and exposure pattern. The height of the raised regions is on the order of 500 Å at maximum. In Fig. 1(b) the mounds do not have a plateau shape; there are protuberances near the edges, showing ''valleys'' sandwiched between the protuberances near the exposure edges. The mounds formed by the exposure with narrower regions, on the other hand, are completely flat on top, and mounds formed by exposure with broader ones show deep and broad ''valleys.'' Moreover, the mound shape concerns with space between exposed regions. Though we can observe various shapes, as like these, the important thing is that the exposed region near the edges increases in height. Hereafter, we refer to the mounds, including the protuberances, as ''hills.''

Figure 2 shows the reflectance line images obtained for four kinds of exposure with different pattern sizes. The reflectance level generally rises on the exposed regions. Here we note two situations. First, the reflectance profiles with protuberances, especially in (a) and (b), correspond fairly well to the topological profiles. Second, the reflectance profiles in (c) and (d) indicate that the exposed region caves in near the center, with high reflectance kept only at the edges. The striking thing is that the degree of ''cave-in'' is occasionally lower than the reflectance level in the unexposed area, as seen in (d). That is, the reflectance decreases in the exposed regions far from the edges. The borderline for the reverse is 30–50 μm from the exposure edges.

Here we mention the influence of hill growth on the surrounding unexposed-regions and hill stability. Figure 3 shows an optical micrograph and some topological profiles

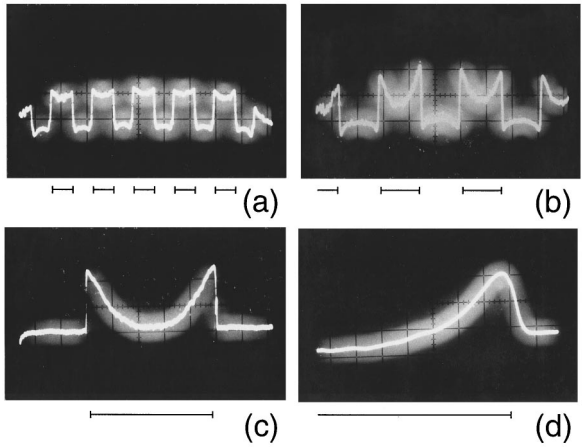

FIG. 2. Pattern dependence of reflectance on the photoexposed $Ag_2Se/GeSe_4$. The measurement was conducted using a He-Ne laser. Horizontal: 10 μm/div; vertical: relative. Lines indicate exposed areas. (a) is for an 8-μm L/S pattern, (b) for a 20-μm L/S pattern, (c) for a 50-μm L/S pattern, and (d) for a 500-μm L/S pattern. The 8-μm L/S pattern means a pattern with 8-μm-wide lines and 8-μm-wide spaces. Likewise for the 20-μm L/S, 50-μm L/S and 500-μm L/S patterns.

of the surfaces where patterned exposures were done twice: a first exposure with a linelike pattern, and a second one while turning the pattern at a right angle. Therefore, some regions were exposed once, others twice, and still others were completely unexposed. As shown in Fig. 3(a), the image becomes progressively darker for the unexposed, the second-exposed, and the first-exposed regions. In Fig. 3(b), comparisons of profile ① with ② and of the profile ③ with ④ show us there are interaction between the first exposure effect and the second one. The hills in profiles ① and ② are the same shape and height. The consequence of the second exposure for the surrounding regions is a poor profile, ③, and the second exposure on the hills results in a flat profile, ④.

Figure 4 shows the exposure dependence of hill growth measured for a hill with a fairly flat top. It is apparent that both the height and the width increase logarithmically with exposure. A very striking finding is that the width extends

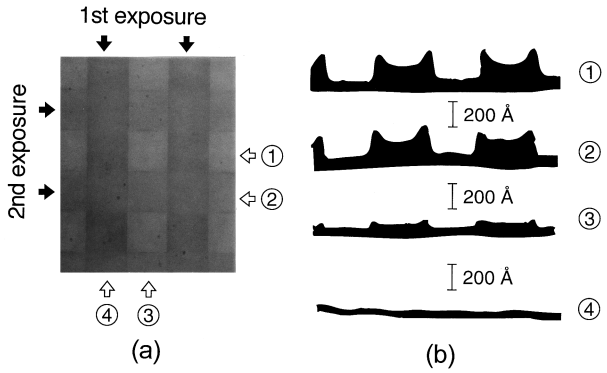

FIG. 3. (a) Optical micrograph showing a transparent image on a doubly exposed $Ag_2Se/GeSe_4$ surface. Following a first exposure through a linelike pattern, a second exposure was performed while turning the structure at a right angle. Black arrows indicate the exposed regions. (b) Surface profiles along the directions indicated by the white arrows (①, ②, ③, and ④) in (a).

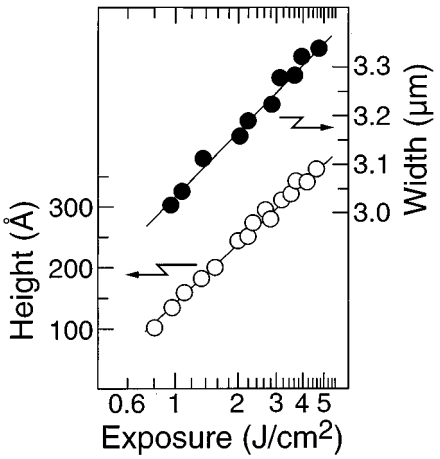

FIG. 4. Exposure dependence of the hill height and hill width. Exposures were done in a 3-μm-wide region. The height and width measurements were conducted using a stylus-type profiler and a SEM, respectively.

beyond the 3-μm-wide exposed region to 3.3 μm at a maximum.

Figure 5 shows typical AES results for the pattern-exposed surface, which were obtained with an exposure region of 10 μm and a unexposure region of 80 μm. The surface has hills about 100 Å in height. The AES images were obtained for Ag and Se elements, whereas no signals were detected for Ge elements on the surfaces either before or after exposure. We see that the exposed area is bright in the image for Ag signal. Note that the bright and shaded areas in the image for the Se signal are the reverse of those for the Ag signal. The AES line profiles illustrate two important features. The first is that exposure remarkably increases the Ag signal intensity, which is accompanied by a lowering of Ag signal intensity in surrounding unexposed regions. The Se signal, in contrast, decreases in the exposed regions, and increases in the surrounding unexposed region. The second feature is that, in the center, the AES spectra for Ag are concave and the spectra for Se are convex. This is more

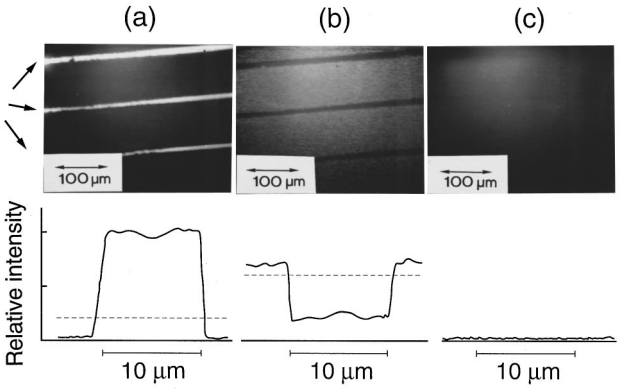

FIG. 5. Auger electron images and line profiles on the $Ag_2Se/GeSe_4$ surface just after patterned photoexposure (4000 mJ/cm^2). (a) is for Ag, (b) for Se, and (c) for Ge. Arrows indicate exposed areas. Dashed lines show each level before exposure. The exposed regions rise to about 100 Å in height, according to the surface topology measurement.

remarkable for exposure with a close-packed L/S pattern. The concave feature in the AES spectra for Ag resembles those in the topological profile and the reflectance line images, as shown in Figs. 1(b) and 2(a). Finally, we should add that occasionally AES signals for Se completely disappeared in the exposed region, being different to the case in Fig. 5(b). This was observed in the exposed region after more prolonged exposure than that in Fig. 5, which produced hills exceeding 300 Å in height.

IV. DISCUSSION

So far, many kinds of photoinduced surface phenomena have been reported. To our knowledge, however, there are no reports on changes in mechanical properties, like the huge change in surface profiles found here. It is obvious that such a giant change cannot be explained by simple lattice relaxation, but only by a movement of large numbers of atoms, i.e., Ag^+ ion movement. Such atom movement would necessarily result in a different material structure to accompany the change in the surface topology. On the other hand, an oblique surface, like the protuberances, should provide low reflectance. The reflectance signals in the measurement system used here do not do so. Therefore, the increase in the reflectance of the hill rather reflects the change in composition caused by exposure. Thus the topological and optical measurements imply photoinduced atom movements, resulting in a new material structure.

From the experimental results mentioned above, a reasonable assumption would be that the hills formed on the pattern-exposed $Ag_2Se/GeSe_4$ surface are composed of Ag-rich compounds. However, we believe the hills are composed of Ag metal in itself. This assertion, which is directly verified by the fact that the 300-Å-high hills shows no AES signals for Se, is in good correspondence to the increase in optical reflectance for the hill (Fig. 2), which means the formation of highly reflective materials, i.e., Ag metal. Unlike in Ag-rich compounds, there are no movable Ag^+ ions in Ag metal. The Ag hills once formed are so stable in nature that they do not lose their shape by subsequent exposure. This is shown by the similarity and the flatness of the topological profiles observed in the double-exposure experiments [Fig. 3(b)]. The AES signal generally reflects only elements 50–100 Å below the surface. So the AES signal for Se in the exposed region in Fig. 5(b) is considered to be from the underlying original Ag_2Se layer.

Some of our results appear to point to Ag^+ ion flow from the unexposed surroundings to the exposed area as the hill formation kinetics. In fact, the AES intensity for Ag around the hill is reduced to a point even lower than that before the exposure, whereas the AES intensity for Se increases because Ag^+ ions disappear and Se atoms remain. That Ag^+ ion flow causes the hill formation is also supported by the profile similarity and the poorness of the profile [Fig. 3(b)]. No hills form in the areas around a hill, indicating the disappearance of the Ag materials from these areas.

It seems that the Ag^+ ions flowing almost immediately change in quality to contribute to form Ag metal. This occurs at exposure edges, which is the reason for the protuberance feature. The concave and convex features in the AES spectra for Ag and Se in Fig. 5 directly show this ''freezing'' of

movable Ag^+ ions. The question is, how long can Ag^+ ions move freely in the exposed region without changing to Ag metal? Judging from the inverse of the reflectance level shown in Figs. 2(c) and 2(d), the distance would be 30–50 μm from the edge at a maximum. The Ag photodoping can be seen only beyond this area. This is because the photodoping results in Ag-doped $GeSe_2$ material, which have a lower reflectance than Ag_2Se. Beyond 50 μm, the hill formation is ordered out of the Ag transport process, and the Ag doping supersedes it. Conversely, if the exposed region is excessively narrow, the Ag^+ ion flow from both sides of the exposure pattern may overlap to form flat-topped hills. The flat-topped hill used in the hill growth measurement (Fig. 4) seems to be due to this.

The lateral Ag^+ ion flux is seemingly from the low Ag concentration area (Ag_2Se layer) to the high one (Ag metal). This is contradictory to the traditional concept of species flow, according to diffusion law. Our explanation for this is that in the exposed region, Ag^+ ions immediately move from the Ag_2Se matrix to its surface, forming the hills. Thus a four-layer structure—(Ag metal)/Ag_2Se/(Ag-doped Ge-Se)/Ge-Se—is possibly formed near the exposure edges. The law of the conservation of mass stands in the Ag_2Se matrix concerning the Ag^+ ions. Thus the diffusion law possibly holds for Ag^+ ion flow in the (Ag metal)/Ag_2Se/(Ag-doped Ge-Se)/Ge-Se system.

The important implication from this structure is that the uppermost Ag hill layer, not the intermediate (Ag-doped Ge-Se) layer, dominantly determines lithography performances of the system when it is used as an etching resist. Up to now a sharp developed pattern has been readily assumed to reflect the existence of sharp Ag-photodoping profiles (the edge sharpening effect).[7,8] So the edge sharpening expected in the developed pattern is mostly due to Ag hill formation, especially as characterized by a protuberance.

We now turn to modeling the Ag-lateral transport in the Ag_2Se layer. So far, the Ag photodoping into the underlying Ge-Se layer has been assumed to be only a driving force for Ag-lateral diffusion.[7,8] Now that this interesting phenomenon of Ag-hill formation has been found, we must rewrite the formula relating to the transport mechanism. Consider the case of photoexposure with an L/S pattern like that in the present experiment. This permits us to discuss a one-dimensional system. Assuming that the process linearly depends on the exposure intensity at the (Ag hill)–Ag_2Se and Ag_2Se–(Ag-doped Ge-Se) interfaces,[9] the mass transport of Ag^+ ions in the Ag_2Se layer can be described as

$$\begin{aligned}\partial C/\partial t = D\partial^2 C/\partial X^2 - I_0(1-R_0)\exp(-\alpha_h l_h)(1-R_h)\\ \times\exp(-\beta_i C)C\eta_d - I_0(1-R_0)\\ \times\exp(-\alpha_h l_h)(1-R_h)C\eta_h ,\end{aligned} \tag{1}$$

where C is the normalized concentration of Ag^+ ions in Ag_2Se, which is a function of position and time $[0\leqslant C(X,t)\leqslant 1]$, D is the diffusivity of Ag^+ ions in Ag_2Se, I_0 is the incident light intensity, R_0 and R_h are optical reflectances in air–(Ag hill) and (Ag hill)–Ag_2Se interfaces, respectively, α_h is the optical-absorption coefficient of the hill, l_h is the hill height, β_i is a parameter related to the optical absorptivity of Ag_2Se, and η_d and η_h are constants related to the sensitivities of the doping and hill formation to photoexposure, respectively. Equation (1) was deduced from considerations of substantial photoexposure at each interface: $I_0(1-R_0)\exp(-\alpha_h l_h)(1-R_h)$ at the (Ag hill)–Ag_2Se interface and $I_0(1-R_0)\exp(-\alpha_h l_h)(1-R_h)\exp(-\beta_i C)$ at the Ag_2Se–(Ag-doped Ge-Se) interface. The first, second, and third terms on the right side of Eq. (1) represent the lateral diffusion, the doping, and the hill formation, respectively. The lateral diffusion results from the latter two terms. The third term has been completely overlooked in the traditional way of thinking, which means that the Ag^+ ion flow mechanism has been mistaken.[7,8] At this point we can say conclusively that the Ag^+ ion flux is correctly analyzed by Eq. (1).

From Eq. (1), the ratio of the doping effect and hill formation effect on the lateral diffusion is expressed as $[\exp(-\beta_i C)\eta_d]/\eta_h$. Assuming $C=l_i/l_{i0}$, where l_{i0} is the initial Ag_2Se thickness and l_i is its thickness as hill formation progresses, and $\beta_i C=\alpha_i l_i$, we obtain $\beta_i=\alpha_i l_{i0}$, where α_i is the absorptivity of Ag_2Se. Setting $l_i=20$ nm and $\alpha_i=2\times10^6$ cm^{-1} at wavelength $\lambda=365$ nm,[10] which conform to the experimental conditions, $\exp(-\alpha_i l_i)$ becomes about 2×10^{-2}. So the intensity of exposure through the Ag_2Se layer becomes very weak. Unfortunately, the exact ratio of η_d/η_h is not known now. However, even assuming that η_d is several dozen times as large as η_h, the hill formation has more of an effect on Ag lateral diffusion than Ag doping does. This seems to be figuratively demonstrated by the hill near the exposed-pattern edges.

Now we turn our attention to the hill growth process. We are concerned with hill formation during exposure with narrow patterns in which the doping effect is seemingly negligible. The increase in hill height, Δl_h, should be in proportion to the decrease in the concentration of Ag^+ ions in Ag_2Se: $\Delta l_h=-k\Delta C$, where k is a constant. Further assume that the decreased concentration near the exposure edges recovers to its original level during photoirradiation, owing to an ample supply of Ag^+ ions from the unexposed regions: $C=1$. They mean all of the incoming Ag^+ ions change into Ag metal. In this case, Eq. (1) reduces to

$$dl_h/dt = kI_0(1-R_0)(1-R_h)\exp(-\alpha_h l_h)\eta_h . \tag{2}$$

Assuming no dependence of reflectance on the hill height, l_h, the hill height is then expressed as

$$l_h(t)=\ln[1+kI_0(1-R_0)(1-R_h)\alpha_h\eta_h t]/\alpha_h . \tag{3}$$

Thus the hill height increases logarithmically with increasing exposure time or the incident light intensity, which is in good accordance with the relation shown in Fig. 4. This suggests that the hill grows as a result of pressure from below caused by Ag metal produced at the (Ag hill)–Ag_2Se interface. If vertically diffused Ag atoms proceed to pile up on the hill surface in succession, the hill height should increase by the square root of time. This does not hold, however, as shown in Fig. 4.

Equation (3) assumes simply that hill formation is linearly dependent on the amounts of radiation incident on the Ag_2Se near the edge. The Ag hill may grow in every direction from the exposure edges. So the above consideration also applies to the logarithmic growth of Ag hill width, corresponding to that in Fig. 4.

The remaining problem is the kinetics of Ag metal formation at the Ag_2Se surface. For Ag/As_3S_7 systems, Owen, Firth, and Zwen proposed a model where a synthetic reaction ($Ag + As_3S_7 \rightarrow AgAsS_2$) is optically induced, resulting in a photodoping effect.[11] Considering that $AgAsS_2$ exhibits *p*-type semiconducting properties, Tanaka, Yushida, and Yamaoka proposed a lateral flow of Ag^+ ions as a countercurrent for the flow of photogenerated holes in the $AgAsS_2$ matrix.[12] In the present work, however, this is not the situation. The hill formation is, seemingly, rather like the decomposition reaction $Ag_2Se \rightarrow Ag + AgSe$. Moreover, the major diffusive motion in the Ag_2Se matrix is that of electrons,[13] implying the importance of photoexcited electrons.

The formation of Ag metal clusters calls to mind latent image formation in photographic silver bromide (AgBr). Some physical factors in latent image formation in AgBr have some resemblance to factors in the present case. One is that the electron mobility in AgBr compounds is higher than the hole mobility.[14] The present Ag_2Se behaves exactly in this manner, as mentioned above. Another is that photographic AgBr is usually sensitized to the surface to form Ag_2S molecules.[14] In the present case, natural ''Ag_2Se molecules'' are expected to exist at the Ag_2Se surface or at the (Ag hill)$-Ag_2Se$ interface. It seems this enables, unlike in photographic AgBr plates, the prompt formation of large Ag metal clusters without chemical development processes. So we can reasonably assume that the Ag hill formation is due to a combination of photoexcited electrons with movable Ag^+ ions.

There is a possible alternative to Eq. (1) for understanding the Ag hill growth. Ample electrons may be photoexcited at the Ag hill surface, rather than at the (Ag hill)$-Ag_2Se$ interface, and then diffuse through the newly formed Ag hill matrix toward the interface. It is provable that the number of these attenuates exponentially to the diffusion length. This is the same as the decrease in photoexposure intensity, shown in Eq. (1). Therefore, combination of photoexcited electrons with movable Ag^+ ions depends logarithmically on exposure intensity. In results, the logarithmic attenuation of photoexcited electron may also explain the features in Fig. 4.

Assuming only the Ag-doping effect, Leung, Newreuther, and Oldham tentatively calculated the distribution of Ag atoms after pattern exposure.[8] How about the actual structure including the Ag hill formation? How the proposed structure—(Ag metal)/Ag_2Se/(Ag-doped Ge-Se)/Ge-Se—is distributed in the exposed regions may depend on the parameters D, R_0, R_h, α_h, β_i, η_d, and η_h is Eq. (1). Unfortunately, their exact values are at present not known at all, so we cannot analytically resolve the equation to exactly exposed area. However, the most important thing is that the (Ag metal)/Ag_2Se/(Ag-doped Ge-Se)/Ge-Se structure is not uniformly distributed in the whole exposure region; whereas the (Ag metal)/Ag_2Se/Ge-Se structure certainly becomes stout near the exposure edges, the (Ag-doped Ge-Se)/Ge-Se structure appears only in the exposure region far from the edges. The implication here is that just the hill formation is the main driving force for Ag-lateral diffusion in the Ag_2Se matrix.

V. CONCLUSION

We have shown that a pattern-photoexposed Ag_2Se/Ge-Se surface exhibits a topological change (hill formation) in addition to the usual photodoping and lateral diffusion effects. The hills are composed of Ag metal resulting from lateral diffusion of mobile Ag^+ ions in the Ag_2Se layer toward the exposed region. The Ag metal growth forms a (Ag metal)/Ag_2Se/(Ag-doped Ge-Se)/Ge-Se structure. The hill formation plays a more dominant role in lateral Ag^+ ion diffusion in the Ag_2Se matrix than photodoping does. The hill formation causes a substantial edge sharpening. The Ag metal formation process is basically similar to the latent image mechanism in photographic silver bromide.

*Electronic address: utsugi@aecl.ntt.co.jp

[1] See, e.g., *Proceedings of the U.S.–Japan Seminar on ''Atomic Processes Induced by Electron Excitation in Non-Metallic Solids'' (Nagoya, Sept. 11–15, 1989)*, edited by W. B. Fowler and N. Itoh (World Scientific, Singapore, 1989).
[2] Y. Utsugi and Y. Mizushima, Jpn. J. Appl. Phys. **31**, 3922 (1992).
[3] Y. Utsugi, Nature (London) **347**, 747 (1990).
[4] A. V. Kolobov and S. R. Elliott, Adv. Phys. **40**, 625 (1991).
[5] Y. Utsugi, A. Yoshikawa, and T. Kitayama, Microelectron. Eng. **2**, 1 (1985).
[6] Y. Utsugi, M. Kakuchi, and H. Maezawa, Rev. Sci. Instrum. **60**, 2295 (1989).
[7] K. L. Tai, E. Ong, R. G. Vadimsky, C. T. Kemmer, and P. M. Bridenbaugh, in *Proceedings of the Symposium on Inorganic Resist Systems*, edited by D. A. Doane and A. Heller (Electrochemical Society, Pennington, NJ, 1982), Vols. 82–9, p. 49.
[8] W. Leung, A. R. Newreuther, and W. G. Oldham, IEEE Trans. Electron Devices, **ED-33**, 173 (1986).
[9] M. Janai, Phys. Rev. Lett. **47**, 726 (1981).
[10] Y. Utsugi, Jpn. J. Appl. Phys. (to be published).
[11] A. E. Owen, A. P. Firth, and P. J. S. Zwen, Philos. Mag. B **52**, 347 (1985).
[12] K. Tanaka, N. Yoshida, and Y. Yamaoka, Philos. Mag. Lett. **68**, 81 (1993).
[13] S. Miyatani and Y. Yokota, J. Phys. Soc. Jpn. **23**, 35 (1967).
[14] J. F. Hamilton, Adv. Phys. **37**, 359 (1988).